

# CoFeB/MgO/CoFeB Magnetic Tunnel Junctions with Low Resistance-Area Product and High Magnetoresistance

H. D. Gan<sup>1\*</sup>, K. Mizunuma<sup>1</sup>, S. Ikeda<sup>1</sup>, H. Yamamoto<sup>1</sup>, K. Miura<sup>2,1</sup>, H. Hasegawa<sup>1</sup>, J. Hayakawa<sup>2</sup>, F. Matsukura<sup>1</sup>, and H. Ohno<sup>1</sup>

<sup>1</sup>Laboratory for Nanoelectronics and Spintorics, RIEC, Tohoku University, Sendai 980-8577, Japan

\*Phone & Fax: +81-22-217-5555 E-mail: hdgan@riec.tohoku.ac.jp

<sup>2</sup>Hitachi Ltd., Advanced Research laboratory,  
1-280 Higashi-koigakubo, Kokubunji-shi, Tokyo 185-8601, Japan

## 1. Introduction

MgO-based magnetic tunneling junctions (MTJs) are important for the development of advanced magnetoresistive random access memories (MRAMs), nonvolatile logics, and hard disk drives due to their giant tunnel magnetoresistance (TMR) ratios [1-6]. At this time, TMR ratios of up to 604% in pseudo-spin valve (PSV) MTJs [7] and 361% in exchange-biased MTJs [8] with resistance area product (RA) of  $10^3$ - $10^4 \Omega\mu\text{m}^2$  have been reported at room temperature (RT). In order to verify operation of MTJ memory cell for gigabit scale MRAMs, it is necessary to develop the fabrication process of deep submicron MTJ with a design of less than 45 nm scale and the MTJs with RA of less than  $10 \Omega\mu\text{m}^2$  [9,10]. The low RA is realized in the MgO barrier thickness range of less than 1 nm. However, when MgO thickness is thin (<4 monolayer), the MgO has amorphous structure, resulting in a low TMR ratio [11]. To realize high TMR ratio for low-RA MTJs, some techniques have been proposed, e.g., Ta getter [9], *in-situ* infrared heat treatment [10] and Mg layer insertion between CoFeB and MgO layers [12]. In this work, we developed microfabrication process of MTJs with junction width of 40 nm, and investigated TMR properties of CoFeB/MgO/CoFeB PSV MTJs with thin MgO barrier and junction size of  $40 \times 80 \sim 40 \times 200 \text{ nm}^2$ .

## 2. Experimental Procedure

Fig. 1(a) shows a schematic diagram of MTJ used here. The MTJs stacking structure of Ta(5)/Ru(10)/Ta(5)/Co<sub>20</sub>Fe<sub>60</sub>B<sub>20</sub>(5)/MgO( $t_{\text{MgO}}$ )/Co<sub>20</sub>Fe<sub>60</sub>B<sub>20</sub>(2,3)/Ta(5)/Ru(5) (in nm) was deposited on thermally oxidized Si wafer by rf-magnetron sputtering. The MgO layer thickness ( $t_{\text{MgO}}$ ) was varied from 0.6 to 0.9 nm. The *in-situ* annealing in the sputtering vacuum chamber was carried out when MgO deposition has been finished. All samples were fabricated using electron-beam (EB) lithography and Ar ion milling. In order to form resist pattern with 40nm scale, the resist pattern height was adjusted to 80~110 nm by diluting commercial EB-resist with thinner. Fig. 1(b) shows a typical scanning electron microscope (SEM) image of a  $40 \times 120 \text{ nm}^2$  MTJ after lift-off process. Junction area was estimated from similar SEM image with various junction sizes. And then the MTJs were annealed at annealing tem-

perature ( $T_a$ ) ranging from 300°C to 450°C in a vacuum of  $10^{-6}$  Torr under a magnetic field of 4 kOe for an hour. The film structures were investigated by high resolution transmission electron microscopy (HRTEM). We measured the TMR ratios of the samples using a dc four-point probe method applying a magnetic field up to 1 kOe.

## 3. Results and Discussion

Typical *R-H* curve for PSV MTJs with a junction size of  $40 \times 120 \text{ nm}^2$  annealed at 400°C is shown in Fig. 2(a). TMR ratio in the MTJ with  $RA=15 \Omega\mu\text{m}^2$  is 275%. A high (low) resistance state, i.e., antiparallel (parallel) magnetization configuration, is stable. It is suggested that the magnetic layers exhibit a single domain-like behavior. In addition,

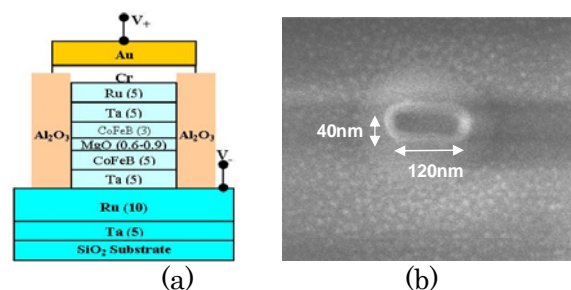


Fig. 1 (a) Schematic drawing of the cross section of the MTJs. (b) SEM image of a  $40 \times 120 \text{ nm}^2$  MTJ.

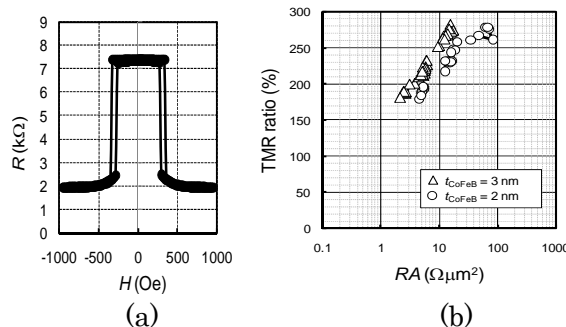


Fig. 2 (a) *R-H* curve for PSV MTJs with a junction size of  $40 \times 120 \text{ nm}^2$ . (b) TMR ratios as a function of RA in MTJs with different thicknesses of MgO barrier and top CoFeB layer.

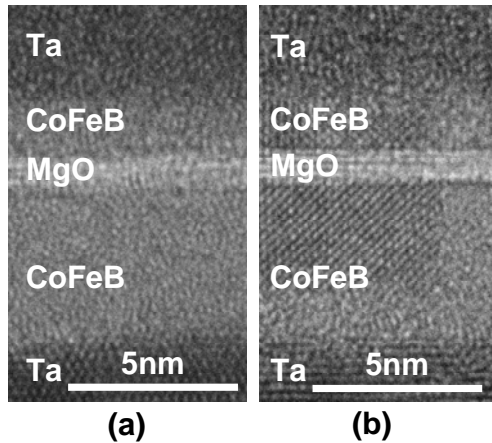


Fig. 3 cross-sectional HRTEM images of Ta(5)/Ru(10)/Ta(5)/Co<sub>20</sub>Fe<sub>60</sub>B<sub>20</sub>(5)/MgO(0.6)/Co<sub>20</sub>Fe<sub>60</sub>B<sub>20</sub>(2)/Ta(5)/Ru(5) (a) before and (b) after annealing at  $T_a=375^\circ\text{C}$ .

the antiparallel configuration in zero magnetic field is caused by the magnetostatic coupling at both ends of the two CoFeB magnetic layers [13]. Fig. 2(b) shows the TMR ratio as a function of  $RA$  at parallel magnetization configuration for MTJs with different top CoFeB thicknesses annealed at  $T_a = 400^\circ\text{C}$ . The TMR ratio increases when CoFeB thickness increases from 2 nm to 3 nm, which may result from magnetic and structural differences in the CoFeB layer accompanying diffusion of Ta. In the MTJs with a 3 nm-thick CoFeB top layer, the TMR ratios reach over 200% in the  $RA$  range of more than  $3 \Omega\mu\text{m}^2$ . We also obtained TMR ratio of 181% at  $2.2 \Omega\mu\text{m}^2$ .

To examine the structure of the thin-MgO-barrier MTJs with low  $RA$ , HRTEM was employed. Fig. 3 presents the cross-sectional HRTEM images for samples consisting of Ta(5)/Ru(10)/Ta(5)/Co<sub>20</sub>Fe<sub>60</sub>B<sub>20</sub>(5)/MgO(0.6)/Co<sub>20</sub>Fe<sub>60</sub>B<sub>20</sub>(2)/Ta(5)/Ru(5) before and after annealing at  $T_a=375^\circ\text{C}$ . In the as-deposited state, the MgO barrier and the Co<sub>20</sub>Fe<sub>60</sub>B<sub>20</sub> electrodes have amorphous structures. At  $T_a=375^\circ\text{C}$ , the amorphous CoFeB/MgO/CoFeB stack crystallized to a highly oriented (001) texture, in accordance with the high TMR ratio owing to coherent tunneling.

In order to improve the crystal quality of ultrathin MgO barrier deposited on the CoFeB layer, *in-situ* annealing at  $350^\circ\text{C}$  right after the deposition of MgO barrier was carried out. The completed MTJ stack was annealed at  $400^\circ\text{C}$ . Fig. 4 shows the TMR ratio as a function of  $RA$  in MTJs with/without  $350^\circ\text{C}$  *in-situ* annealing. For the MTJs with *in-situ* annealing, high TMR ratios were observed in the lower  $RA$  range. The TMR ratio of 122% with  $RA=1.0 \Omega\mu\text{m}^2$ , TMR ratio of 132% with  $RA=1.1 \Omega\mu\text{m}^2$ , and TMR ratio of 152% with  $RA=1.3 \Omega\mu\text{m}^2$  were obtained.

#### 4. Conclusions

We developed microfabrication process of MTJs with junction width of 40 nm, and investigated TMR properties of CoFeB/MgO/CoFeB PSV MTJs with thin MgO barrier and junction size of  $40\times 80\sim 40\times 200 \text{ nm}^2$ . The TMR ratio

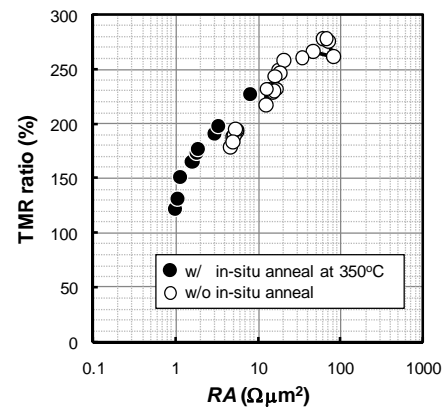


Fig. 4 TMR ratios as a function of  $RA$  in MTJs with/without  $350^\circ\text{C}$  *in-situ* annealing. The MTJs were post-annealed at  $400^\circ\text{C}$ .

increases with increasing annealing temperature and reaches over 200% in the  $RA$  range of more than  $3 \Omega\mu\text{m}^2$ . We also obtained TMR ratio of 122% at  $RA=1.0 \Omega\mu\text{m}^2$  by *in-situ* annealing.

#### Acknowledgements

This work was supported by “High-Performance Low-Power Consumption Spin Devices and Storage Systems” program under Research and Development for Next-Generation Information Technology of MEXT. The authors wish to thank Y. Ohno, K. Ohtani, I. Morita, and T. Hirata for their valuable discussions and technical support in MTJ fabrication.

#### References

- [1] S. Yuasa *et al.*, Nat. Mater. **3** (2004) 868.
- [2] S. S. Parkin *et al.*, Nat. Mater. **3** (2004) 862.
- [3] D. D. Djayaprawira *et al.*, Appl. Phys. Lett. **86** (2005) 092502.
- [4] J. Hayakawa *et al.*, Jpn. J. Appl. Phys. **44** (2005) L587.
- [5] T. Kawahara *et al.*, IEEE J. Solid-State Circuits **43** (2008) 109.
- [6] S. Matsunaga *et al.*, Appl. Phys. Express **1** (2008) 091301.
- [7] S. Ikeda *et al.*, Appl. Phys. Lett. **93** (2008) 082508.
- [8] Y. M. Lee *et al.*, Appl. Phys. Lett. **89** (2006) 042506.
- [9] Y. Nagamine *et al.*, Appl. Phys. Lett. **89** (2006) 162507.
- [10] S. Isogami *et al.*, Appl. Phys. Lett. **93** (2008) 192109.
- [11] S. Yuasa *et al.*, Appl. Phys. Lett. **87** (2005) 242503.
- [12] K. Tsunekawa *et al.*, Appl. Phys. Lett. **87** (2005) 072503.
- [13] W. Folkerts, J. Magn. Magn. Mater. **94** (1991) 302.